Received: 27 January 2023 | Revised: 7 April 2023 | Accepted: 21 July 2023

DOI: 10.1002/cac2.12474

CANCER COMMUNICATIONS Open Access

LETTER TO THE EDITOR

Novel CD123×CD33 bicistronic chimeric antigen receptor (CAR)-T therapy has potential to reduce escape from single-target CAR-T with no more hematotoxicity

Dear Editor,

Antigen escape is responsible for resistance [1] or disease relapse [2] from single-target chimeric antigen receptor (CAR)-T therapy. Dual-target CAR-T therapy has the potential to overcome the escape problem. However, the efficacy and safety assessment of dual-target CAR-T therapy in treating acute myeloid leukemia (AML) need further investigation. Tandem CAR-T therapy has been widely used in research and clinic. However, clustering of two connected single-chain variable fragments (scFvs) [3] and the inappropriate conjugation distance [4] pose a risk of damaging tandem CAR-T cells' function. Moreover, the bicistronic approach has been proven to be more efficacious than tandem and pooled approaches in treating multiple myeloma [5]. Both CD33 and CD123 are regarded as ideal AML targets, and simultaneously targeting CD33 and CD123 can treat almost all AML patients. Therefore, we developed a CD123×CD33 bicistronic CAR (123×33 biCAR) whose scFvs differed from any existing one to improve the clinical efficacy and to explore its hematotoxicity (Supplementary Materials and Methods), as the only published preclinical study of 123×33 biCAR, designed with different scFvs and vectors, did not assess its safety [6].

The 123×33 biCAR-T cell was designed to cope with the antigen escape problem by expressing fully functional anti-CD123 CAR (123CAR) and anti-CD33 CAR (33CAR) in one T cell (Figure 1A). Two second-generation CARs containing 4-1BB/CD3-ζ intracellular signaling components were linked by T2A sequence and cloned into a lentiviral backbone to obtain the bicistronic CAR vector (Figure 1B). CD123 scFv and CD33 scFv were derived from clone 13C3 and clone HI33a, respectively, both of which were established by our laboratory. Flow cytometry (FCM) analysis showed that both 123CAR and 33CAR were highly expressed (above 40.0%) on T cell surface (Figure 1C).

Co-culture test showed that 123×33 biCAR-T cells lysed not only $CD123^+CD33^+$ Molm13 cells but also $CD123^-CD33^+$ Jurkat (Jurkat33) or $CD123^+CD33^-$ Jurkat (Jurkat123) cells; in comparison, 123CAR-T or 33CAR-T cells did not lyse Jurkat cells without corresponding antigen; none of three types of CAR-T cells exhibited cytotoxicity toward $CD123^-CD33^-$K562 cells (Figure 1D, Supplementary Figures S1-S2). Enzyme-linked immunosorbent assay (ELISA) test showed that 123×33 biCAR-T cells released high levels of interferon-γ (IFN-γ) and tumor necrosis factor-α (TNF-α) against Molm13, Jurkat123 and Jurkat33 cell lines, which were hundreds to thousands folds of that secreted by normal T cells (Supplementary Figure S3). The above data indicated that 123×33 biCAR-T cells have specific cytotoxicity against either CD123 or CD33 in vitro.

Two xenograft mouse models were established to evaluate the in vivo efficacy of 123×33 biCAR-T cells. Firstly, a Molm13-NOD/SCID/IL2Rγ-/- (NSG) model was established (Supplementary Figure S4) to mimic the most common situations in AML patients, where CD123 and CD33 are usually expressed concomitantly. The 123×33 biCAR-T performed as well as or better than single-target CAR-T in eradicating Molm13 cells (Figure 1E,

Abbreviations: CAR, chimeric antigen receptor; AML, acute myeloid leukemia; scFvs, single chain variable fragments; 123×33 biCAR, CD123×CD33 bicistronic CAR; FCM, flowcytometry; ELISA, enzyme-linked immunosorbent assay; IFN-γ, interferon-γ; TNF-α, tumor necrosis factor-α; NSG, NOD/SCID/IL2Rγ-/-; FDR, false discovery rate; TGF-β, transforming growth factor-β; PI3K-AKT-mTOR, phosphatidylinositol 3-kinase/protein kinase B/mammalian target of rapamycin; HSPCs, hematopoietic stem and progenitor cells; scRNA-seq, single-cell RNA-sequencing; UMAP, uniform Manifold Approximation and Projection; HSC, hematopoietic stem cell; MPP, multipotent progenitors; MEP, megakaryocyte-erythroid progenitors; GMP, granulocyte-monocyte progenitors; MLP, multi-lymphoid progenitors; GSEA, gene set enrichment analysis; CFU, colony forming units; BFU-E, burst-forming unit-erythroid; CFU-E, colony-forming unit-erythroid; CFU-M, colony-forming unit- megakaryocyte; BLI, Bioluminescent imaging.

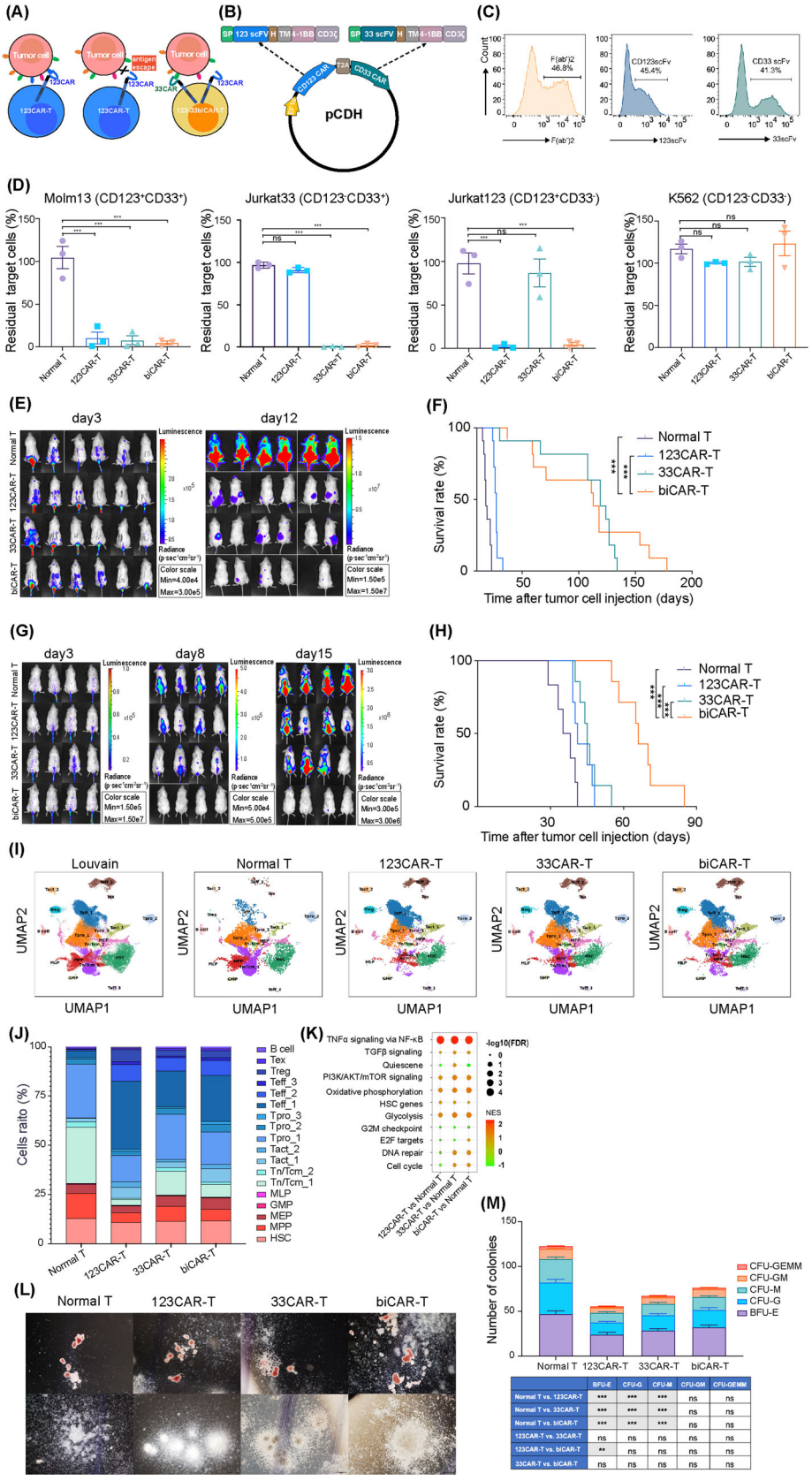

FIGURE 1 Structure and biological properties of 123×33 biCAR-T. (**A**) Antigen losing or switching leads to tumor escape, and 123×33 biCAR-T cells overcome this issue by specifically targeting both antigens simultaneously. **(B)** Schematic diagram of the 123×33 biCAR. 13C3 scFv was incorporated with the 4-1BB/CD3ζ signaling domain to generate a second-generation CAR. CD123 and CD33 CARs were linked via a T2A sequence and cloned into a pCDH vector. **(C)** CAR expression was detected using FCM. Human recombinant CD123 and CD33 proteins were used to detect the expression of each CAR. $F(ab')_2$ positive cells represent CAR^+ cells. **(D)** Representative histograms depicting the

Supplementary Figure S5) and prolonging the Molm13-NSG mice survival time (Figure 1F). In addition, an antigen escape model was established by engrafting NSG mice with a mixture of equal number of Jurkat123 and Jurkat33 cells (Supplementary Figure S6). In this Jurkat hybrid model, 123×33 biCAR-T cells showed obvious superiority over the two types of single-target CAR-T cells in suppressing tumor burden (Figure 1G, Supplementary Figure S7) and prolonging survival time (Figure 1H), substantiating the advantage of dual-target CAR in antigen-loss situations. The two main possible reasons for the non-durable anti-leukemia effect in vivo in our study are the rejection of mice against human T cells and limited amount of CAR-T cells in vivo, which was lower than the number reported in the other literature [7]. All things considered, 123×33 biCAR-T cells showed robust anti-AML effect and promising anti-escape capacity in vivo.

The off-target cytotoxicity of 123CAR and 33CAR on normal hematopoietic stem and progenitor cells (HSPCs) has been controversial [7-9]. Herein, we first evaluated the influence of 123×33 biCAR on hematopoiesis by several methods. Cord blood-derived $CD34^+$ cells were co-cultured with normal T or CAR-T cells in a 1:1 ratio for 24 h. Although enhanced cytokine secretion (Supplementary Figure S8) was observed in CAR-T groups, none of the three types of CAR-T cells induced a significant reduction in $CD34^+$ cell counts (Supplementary Figure S9) compared to normal T cells, which indicated that CAR-T cells in this study had no obvious specific cytotoxicity against $CD34^+$ cells in vitro.

Additionally, single-cell RNA-sequencing (scRNA-seq) analysis was performed to better understand the effect of CAR-T cells on HSPCs. Reduced dimension analysis using Uniform Manifold Approximation and Projection (UMAP) visualization showed 18 distinct clusters (Figure 1I). The cell type was annotated in each cluster in the UMAP plot, and five clusters located in the lower part of the plot were identified as HSPCs: hematopoietic stem cells (HSCs), multipotent progenitors (MPPs), megakaryocyte-erythroid progenitors (MEPs), granulocyte-monocyte progenitors (GMPs), and multi-lymphoid progenitors (MLPs). HSCs and MPPs (Figure 1I-J, Supplementary Figure S10) constituted the majority of HSPCs. The proportion of the HSC subpopulation barely changed among the groups (12.8%, 10.8%, 11.5% and 11.7% in normal T, 123CAR-T, 33CAR-T and 123×33 biCAR-T groups, respectively), while the MPP subpopulation was reduced in CAR-T groups (12.7%, 4.9%, 7.6% and 5.9% in normal T, 123CAR-T, 33CAR-T and 123×33 biCAR-T groups, respectively) (Figure 1J). Therefore, CAR-T cells reduced progenitor cells, but not stem cells, in vitro.

The results of Gene Set Enrichment Analysis (GSEA) revealed that the enrichment of quiescence, cell cycle, G2M checkpoint and E2F target-related genes was not altered in the HSC subpopulation by CAR-T cells (Figure 1K, Supplementary Figure S11 Supplementary Table S3). In addition, downregulation of the transforming growth factor (TGF)-β signaling pathway or enrichment of the phosphatidylinositol 3-kinase/protein kinase B/mammalian target of rapamycin (PI3K-AKT-mTOR)

proportion of the residual target cells Molm13, Jurkat33, Jurkat123 and K562 after co-culture with CAR-T cells at an E:T ratio of 1:1 for 24 h. (n = 3; mean ± SEM; one-way ANOVA with Dunnett's multiple comparison test; ns, no significance; ***$P < 0.001$). **(E)** BLI of luciferase activity in NSG mice on days 3 and 12 after inoculation of Molm13 cells (n = 6 mice per group, one from the 123×33 biCAR group died of anesthesia on day 3). **(F)** Kaplan–Meier survival curves for the overall survival of the Molm13-inoculated mice (n = 11; log-rank test; *** $P < 0.001$). Survival observation was conducted independently from BLI to avoid the negative effect of anesthetic injection on mice survival. **(G)** BLI of Jurkat123- and Jurkat33-inoculated mice from the different treatment groups (n = 4 mice per group) on the indicated days. **(H)** Kaplan–Meier survival curves for the overall survival of the Jurkat123- and Jurkat33-inoculated mice (n = 7 in each CAR-T group, and n = 6 in the normal T group; log-rank test; *$P < 0.05$; ***$P < 0.001$). Survival observation was conducted independently from BLI to avoid the negative effect of anesthetic injection on mice survival. **(I-K)** scRNA-seq analysis of residual $CD34^+$ cells treated with different T/CAR-T cells. **(I)** UMAP visualization indicating 0 –17 clusters identified based on single-cell transcriptomes. Cell type was annotated on the corresponding cluster. Each dot represents a single cell, and colors indicate cell clusters. **(J)** Stacked bar plots indicating the frequencies of defined cell types in different samples. Hematopoietic cells are marked in various tones of red, and T cells are shown in different tones of blue. **(K)** Dot plot of GSEA results of HSC in different CAR-T groups compared with HSC in normal T group based on the indicated gene sets. **(L-M)** CFU assay to determine the colony-forming ability of residual $CD34^+$ cells of different groups. **(L)** Representative photos of colonies in different groups. **(M)** Histogram showing the colony numbers of each group. (n = 3; mean ± SEM; P values were calculated by two-way ANOVA with Dunnett's multiple comparison test and are shown in the table below the graphs; ns, no significance; *** $P < 0.001$).

Abbreviations: CAR, chimeric antigen receptor; 123×33 biCAR, CD123×CD33 bicistronic CAR; scFvs, single chain variable fragments; FCM, flowcytometry; E:T, effector cell: target cell; SEM, Standard Error of the Mean; Analysis of Variance (ANOVA); BLI, bioluminescent imaging; NSG, nonobese diabetic/severe combined immunodeficiency /IL2Rγ-/-; scRNA-seq, single-cell RNA-sequencing; UMAP, uniform manifold approximation and projection; Teff, effector T cells; Tex, exhausted T cells; Tpro, proliferating T cells; Tact, activated T cells; Tn/Tcm, naïve T/central memory T cells; GSEA, gene set enrichment analysis; HSC, hematopoietic stem cell; CFU, colony forming units; CFU-GEMM, CFU-granulocyte, erythrocyte, macrophage, megakaryocyte; CFU-GM, CFU-granulocyte, macrophage; CFU-M, CFU- macrophage; CFU-G, CFU-granulocyte; BFU-E, burst-forming unit-erythroid.

signaling pathway in the HSC subpopulation treated with CAR-T cells was not observed (Figure 1K, Supplementary Figure S11). Taken together, GSEA indicated that 123×33 biCAR-T cells did not significantly alter the stemness of the HSC cluster.

Colony forming unit (CFU) assays showed similar amount of hematopoietic colonies grown after three types of CAR-T treatment, which were lower than that in the normal T group (Figure 1L-M). It corroborated the results of scRNA-seq and suggested that alive HSPCs on exposure to CAR-T cells targeting CD123 and/or CD33 can differentiate into multiple lineages of blood cells.

Most researchers hold that CD123 [8] or CD33 single-target CAR-T therapy [9] has low toxicity against hematopoiesis, while a minority hold the opposite view [7]. Our results suggested that CAR-T therapies targeting CD123 and/or CD33 were not myeloablative, and scRNA-seq proved that HSCs were exempted and thus probably retained much hematopoietic capacity. Considering the CAR design was not peculiar to our study, the novel scFvs might be the critical factor of the safety profile we observed. Similar findings of Mardiros et al. [8] support this hypothesis, and further studies are needed to explore the mechanism via which scFvs impact the safety of CAR-T cells. Moreover, the concomitant expression of CD123 and CD33 on HSPCs [10] might be one reason why 123×33 biCAR-T cells bring no additional hematotoxicity compared to CD123 or CD33 single-target CAR-T cells.

In conclusion, we constructed a novel 123×33 biCAR-T therapy that has great potential to reduce failure or relapse from single-target CAR-T therapy and proved that it has no more hematotoxicity than CD123 or CD33 single-target CAR-T therapy, which provides more data reference for the preclinical and clinical research of CAR-T therapy targeting both CD123 and CD33.

DECLARATIONS

AUTHOR CONTRIBUTIONS

Zhenzhen Wang designed and optimized the experiments, analyzed the data, and wrote the manuscript. Yang Lu designed and performed the antibody development and screening experiments and analyzed the related data. Yu Liu designed and operated the supplementary experiment to test cytotoxicity of CAR-T cells on $CD34^+$ cells. Junli Mou performed the animal experiments, CFU test, and single-cell sample preparation. Xiaoyu Liu and Manling Chen contributed to animal experiments. Shaowei Qiu, Bing Wang, and Wei Qi analyzed the scRNA-seq data. YingXi Xu, Qing Rao, Haiyan Xing, Kejing Tang, Zheng Tian and Ying Wang contributed to the discussion of project results and provided feedback on the manuscript. Jianxiang Wang, Dongsheng Xiong, and Shaowei Qiu conceptualized the study. Jianxiang Wang, Dongsheng Xiong, Shaowei Qiu and Min Wang assisted with the review and editing of the manuscript and supervised the study and manuscript preparation. All authors have reviewed the final version of the manuscript.

ACKNOWLEDGEMENTS

We would like to thank Dr. Shuo Zhang (State Key Laboratory of Experimental Hematology, Institute of Hematology and Blood Diseases Hospital, Chinese Academy of Medical Sciences and Peking Union Medical College, Tianjin, China) for her help and training in colony forming units related experiments.

CONFLICT OF INTERESTS STATEMENT

The authors declare no conflict of interest.

FUNDING INFORMATION

This work was supported by the National Key Research and Development Program of China (2021YFC2500300), the National Natural Science Foundation of China (81830005), Haihe Laboratory of Cell Ecosystem Innovation Fund (HH22KYZX0032) and the Chinese Academy of Medical Sciences (CAMS) Innovation Fund for Medical Sciences (2020-I2M-C&T-A-019).

ETHICS APPROVAL AND CONSENT TO PARTICIPATE

The study was conducted according to the Declaration of Helsinki and was approved by the ethical advisory board of the Institute of Hematology and Blood Diseases Hospital and Ethics Committee of Haihe Laboratory of Cell Ecosystem. (permit number: HHL2022009-EC-1). Written informed consent was obtained from all the participants. All animal experiments were approved in accordance with the guidelines of the Ethics Committee of Haihe Laboratory of Cell Ecosystem (permit number: HHL2022009-EC-1).

CONSENT FOR PUBLICATION

Not applicable.

DATA AVAILABILITY STATEMENT

Original data will be available via email to the corresponding author at wangjx@ihcams.ac.cn. The raw sequence data reported in this paper have been deposited in the Genome Sequence Archive in National Genomics Data Center, China National Center for Bioinformation / Beijing Institute of Genomics, Chinese Academy of Sciences (GSA-Human: HRA004513) that are publicly accessible at https://ngdc.cncb.ac.cn/gsa-human.

Zhenzhen Wang[1]
Yang Lu[1]
Yu Liu[1]
Junli Mou[1]
Xiaoyu Liu[1]
Manling Chen[1]
Ying Wang[1]
Yingxi Xu[1]
Qing Rao[1]
Haiyan Xing[1]
Kejing Tang[1]
Zheng Tian[1]
Bing Wang[2]
Wei Qi[2]
Min Wang[1]
Shaowei Qiu[1]
Dongsheng Xiong[1]
Jianxiang Wang[1]

[1]*State Key Laboratory of Experimental Hematology, National Clinical Research Center for Blood Diseases, Tianjin Key Laboratory of Cell Therapy for Blood Diseases, Haihe Laboratory of Cell Ecosystem, Institute of Hematology and Blood Diseases Hospital, Chinese Academy of Medical Sciences and Peking Union Medical College, Tianjin, P. R. China*
[2]*Novogene Co, Ltd, Beijing, P. R. China*

Correspondence
Jianxiang Wang, M.D., Dongsheng Xiong, M.D, and Shaowei Qiu, M.D, State Key Laboratory of Experimental Hematology, National Clinical Research Center for Blood Diseases, Tianjin Key Laboratory of Cell Therapy for Blood Diseases, Haihe Laboratory of Cell Ecosystem, Institute of Hematology and Blood Diseases Hospital, Chinese Academy of Medical Sciences and Peking Union Medical College, Tianjin 300020, P. R. China, 288 Nanjing Road, Tianjin, China.
E-mail: wangjx@ihcams.ac.cn, dsxiong@ihcams.ac.cn and qiushaowei@ihcams.ac.cn

Zhenzhen Wang, Yang Lu and Yu Liu contributed equally.

ORCID
Jianxiang Wang https://orcid.org/0000-0001-9437-9151

REFERENCES

1. Lamba JK, Chauhan L, Shin M, Loken MR, Pollard JA, Wang YC, et al. CD33 Splicing Polymorphism Determines Gemtuzumab Ozogamicin Response in De Novo Acute Myeloid Leukemia: Report From Randomized Phase III Children's Oncology Group Trial AAML0531. J Clin Oncol. 2017;35(23):2674–82.
2. Sotillo E, Barrett DM, Black KL, Bagashev A, Oldridge D, Wu G, et al. Convergence of Acquired Mutations and Alternative Splicing of CD19 Enables Resistance to CART-19 Immunotherapy. Cancer Discov. 2015;5(12):1282–95.
3. Ajina A, Maher J. Strategies to Address Chimeric Antigen Receptor Tonic Signaling. Mol Cancer Ther. 2018;17(9):1795–815.
4. Zah E, Lin MY, Silva-Benedict A, Jensen MC, Chen YY. T Cells Expressing CD19/CD20 Bispecific Chimeric Antigen Receptors Prevent Antigen Escape by Malignant B Cells. Cancer Immunol Res. 2016;4(6):498–508.
5. de Larrea CF, Staehr M, Lopez AV, Ng KY, Chen Y, Godfrey WD, et al. Defining an Optimal Dual-Targeted CAR T-cell Therapy Approach Simultaneously Targeting BCMA and GPRC5D to Prevent BCMA Escape-Driven Relapse in Multiple Myeloma. Blood Cancer Discov. 2020;1(2):146–54.
6. Petrov JC, Wada M, Pinz KG, Yan LE, Chen KH, Shuai X, et al. Compound CAR T-cells as a double-pronged approach for treating acute myeloid leukemia. Leukemia. 2018;32(6):1317–26.
7. Baroni ML, Sanchez Martinez D, Gutierrez Aguera F, Roca Ho H, Castella M, Zanetti SR, et al. 41BB-based and CD28-based CD123-redirected T-cells ablate human normal hematopoiesis in vivo. J Immunother Cancer. 2020;8(1):e000845.
8. Mardiros A, Dos Santos C, McDonald T, et al. T cells expressing CD123-specific chimeric antigen receptors exhibit specific cytolytic effector functions and antitumor effects against human acute myeloid leukemia. Blood. 2013;122(18):3138–48.
9. Wang QS, Wang Y, Lv HY, et al. Treatment of CD33-directed chimeric antigen receptor-modified T cells in one patient with relapsed and refractory acute myeloid leukemia. Mol Ther 2015;23(1):184–91.
10. Haubner S, Perna F, Kohnke T, Schmidt C, Berman S, Augsberger C, et al. Coexpression profile of leukemic stem cell markers for combinatorial targeted therapy in AML. Leukemia. 2019;33(1):64–74.

SUPPORTING INFORMATION

Additional supporting information can be found online in the Supporting Information section at the end of this article.